Tunable and precise miniature lithium heater for point-of-care applications

Buddhisha Udugama[a,b,1], Pranav Kadhiresan[a,b,1], and Warren C. W. Chan[a,b,c,d,2]

[a]Institute of Biomaterials and Biomedical Engineering, University of Toronto, Toronto, ON M5S 3G9, Canada; [b]Terrence Donnelly Center for Cellular and Biomolecular Research, University of Toronto, Toronto, ON M5S 3E1, Canada; [c]Department of Chemistry, University of Toronto, Toronto, ON M5S 3H6; and [d]Materials Science and Engineering, University of Toronto, Toronto, ON M5S 3G9, Canada

Edited by Catherine J. Murphy, University of Illinois at Urbana–Champaign, Urbana, IL, and approved January 8, 2020 (received for review September 26, 2019)

Point-of-care diagnostic assays often involve multistep reactions, requiring a wide range of precise temperatures. Although precise heating is critical to performing these assays, it is challenging to provide it in an electricity-free format away from established infrastructure. Chemical heaters are electricity-free and use exothermic reactions. However, they are unsuitable for point-of-care multistep reactions because they sacrifice portability, have a narrow range of achievable temperatures, and long ramp-up times. Here we developed a miniature heater by modulating the lithium–water reaction kinetics using bubbles in a channel. Our heaters are up to 8,000 times smaller than current devices and can provide precise (within 5 °C) and tunable heating from 37 °C to 65 °C (ΔT_{RT} = 12 °C to 40 °C) with ramp-up times of a minute. We demonstrate field portablity and stability and show their use in an electricity-free multistep workflow that needs a range of temperatures. Ultimately, we envision providing better access to cutting edge biochemical techniques, including diagnostics, by making portable and electricity-free heating available at any location.

chemical heater | diagnostics | point of care

Point-of-care diagnostic assays often involve complex multistep reactions that require a wide variety of temperatures for steps ranging from sample processing to genetic analysis (1–3). Although precise heating is critical to running these assays, it is challenging to provide it in field settings away from established infrastructure. Existing methods that provide precise heating such as thermocyclers often rely on electricity. However, electrification rates in resource-poor settings can be as low as 10%, and power outages can leave consumers without access to electricity for over 50% of the hours annually (4, 5). In order to ensure point-of-care diagnostic utilization in such areas, it is paramount that reliance on infrastructure and electricity is minimized (6, 7).

Chemical heaters are an electricity-free solution to providing precise heating for diagnostic assays. Generally, these heaters utilize an exothermic reaction coupled with a phase change material (PCM) and insulation to achieve the required temperature (8–13). However, these heaters are unsuitable for conducting multistep reactions at the point of care. They sacrifice portability, have narrow ranges of achievable temperatures, and long ramp-up times that increase overall turnaround times. While a single temperature is useful for employing a specific enzyme, enzymatic reactions that diagnostics assays leverage span a range of temperatures (14): from restriction endonucleases such as EcoR I performing optimally at 37 °C (15) to *Bst* DNA polymerase performing optimally at 65 °C (16). These chemical heaters are therefore either limited to single-step assays that only require a single temperature, or require multiple chemical heaters tuned to each required temperature. Multiple heaters however are a challenge to implement given their size (9, 17) (up to 4,400 cm^3) and ramp-up times (8) (from 5 to 30 min). In order to use chemical heaters for precise electricity-free heating, it is necessary to reduce the overall size and improve flexibility: both in terms of turnaround time as well as achievable temperatures. Here, we have developed an up to 8,000 times smaller miniature heater using lithium and hydrogen bubble motion in tubes of different shapes.

Our heater uses the interplay between an active chemical reaction and passive bubble flow to harness the energy from an otherwise unpredictable and reactive alkali metal. Lithium was chosen as a fuel source for the heater due to its high energy density (~222 kJ/mole), ease of malleability, and simple activation with water (18). Lithium's malleable nature allows for ease of controlling the shape and surface area of the alkali metal to provide predictable heating. This allowed us to compress the lithium into a channel where the lithium–water reaction could occur and act as a heater. Furthermore, the channel provides an enclosed space where aqueous reactants and gaseous products compete to occupy space within the system. We leveraged the body of research on bubble motion in elongated tubes (19–21) to control the interaction between the reactants to develop reproducible and precise miniature heaters. By harnessing the high specific energy provided by lithium in a controlled manner, we were able to design a heater ideal for the point of care. This development can expedite the translation of complex biological assays to the point of care, with its applicability extending to biological applications such as gene editing (22) or protein synthesis (23, 24).

Significance

Biochemical techniques are required for a variety of different point-of-care applications, from diagnosing illnesses to manufacturing vaccines. Many of these applications cannot be used in remote locations due to their reliance on electricity for temperature control. Here we have developed a miniature lithium heater, up to 8,000 times smaller than existing technologies, enabling the use of biochemical techniques at the point of care. By using these heaters in a model workflow that detects the presence of a virus, we demonstrate their applicability to a broad range of biochemical techniques that require precise temperature control. This technology may be broadly used, such as in disaster relief camps or mountain expeditions, for diagnostic and therapeutic applications.

Author contributions: B.U., P.K., and W.C.W.C. designed research; B.U. and P.K. performed research; B.U. and P.K. contributed new reagents/analytic tools; B.U. and P.K. analyzed data; and B.U., P.K., and W.C.W.C. wrote the paper.

Competing interest statement: We are considering filing a patent on the technology. W.C.W.C. is also associated with Luna Nanotech, a nanoparticle company.

This article is a PNAS Direct Submission.

[1]B.U. and P.K. contributed equally to this work.

[2]To whom correspondence may be addressed. Email: warren.chan@utoronto.ca.

This article contains supporting information online at https://www.pnas.org/lookup/suppl/doi:10.1073/pnas.1916562117/-/DCSupplemental.

First published February 18, 2020.

Results

Development of Miniature Lithium Heaters. To provide portable and electricity-free heating at the point of care, we developed a miniature heater that can fit on a fingertip by harnessing the exothermic reaction of lithium and water. We controlled the temperatures within the heater by modulating the interactions between the reactants, lithium and water, and the products, hydrogen bubbles and lithium hydroxide (Fig. 1*A*). This modulation was achieved by controlling the interface between the two reactants for heating and storage. First, to control this interface for heating, we filled an acrylic channel with lithium. More specifically, we modulated lithium's access to water and controlled the clearance of hydrogen bubbles by varying the channel size and shape and surface tension of water. Next, we controlled the interface between lithium and water vapor in the air for storage, by adding a protective barrier. As lithium is highly reactive with moisture in the air (18), we wanted to ensure that our heaters performed reproducibly even after shipping and storage. We controlled the lithium–water vapor interaction by adding a soluble mixture of excipients, which included mineral oil (25) and mannitol (26, 27), as a barrier for protection. Our miniature heater is comprised of a two-part system: 1) a lithium-filled acrylic channel and 2) a soluble mixture of mineral oil and mannitol (Fig. 1 *B* and *C*). We fabricated this system using a workflow that used laser cutting technology as well as manual compression. First, we laser cut acrylic channels of different sizes and shapes. This was followed by compressing lithium into the laser-cut acrylic molds. We visually inspected the heaters to ensure the lithium is compressed completely to the edges of the channel (*SI Appendix*, Fig. S1). We then sealed one end of the

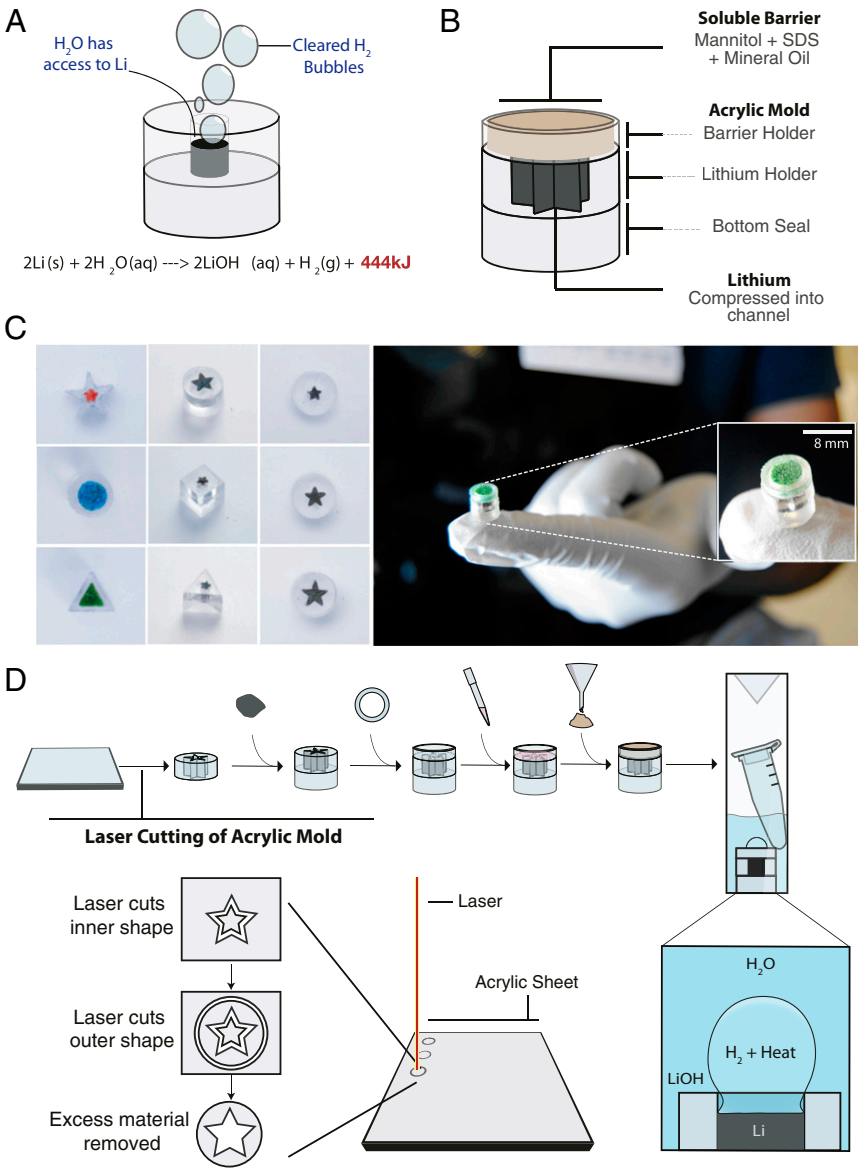

Fig. 1. Development of miniature lithium heaters. (*A*) Schematic depicting the exothermic reaction between lithium and water in a miniature heater. The heaters are designed to control the interactions between the reactants and products of the lithium–water reaction. (*B*) The miniature lithium heaters are comprised of two parts: 1) a lithium-filled acrylic mold and 2) a soluble mixture of powders. (*C*) Photograph of the miniature heater. The heaters can be manufactured to different configurations, while having a footprint that is small enough to fit on a fingertip. (Scale bar, 8 mm.) (*D*) The heaters are developed by first laser cutting the acrylic molds, followed by compression of lithium and sealing of one side of the heater. To this design, stabilizing excipients are added on top of the heater. The miniature heaters can be used to heat reaction tubes that are placed in small volumes of water.

lithium-filled molds with an acrylic sheet base. Lastly, we fitted the other end with a ring-shaped mold to which we added mineral oil, mannitol, and other excipients. After development, we can use the heaters by placing them in 1 to 3 mL of water, which acts as both a reactant and a heat transfer medium to heat reaction tubes (Fig. 1*D*). We chose acrylic as the housing for lithium due to its low thermal expansion coefficient of 75×10^{-6} m/m/K in order to minimize the effect of heat on the dimensions and morphology of the channel (*SI Appendix*, Table S1). We can color code the heaters or vary the shape and size of the acrylic mold, to improve usability for performing a multistep assay requiring multiple heaters (Fig. 1*C*). Here, we demonstrate the development of a miniature heater by using the motion of elongated bubbles in tubes of different shapes to predictably harness the energy from a high energy density alkali metal. By developing an electricity-free heater that can fit on a fingertip, we have designed an infrastructure-independent platform that is highly portable and easy to ship and handle.

Providing Precise and Tunable Temperatures. We wanted to develop a heater that can provide temperatures in the range of 37 °C and 65 °C (ΔT_{RT} = 12°C to 40 °C) with 5 °C of precision. We chose these design criteria based on what is typically required for optimal performance of an enzymatic assay (*SI Appendix*, Table S2). Precise and tunable heating was achieved by varying the shape and surface area, respectively, of the acrylic channels of the heater. We used a simpler version of the miniature heater to systematically determine the effect of shape and surface area on the precision and tunability of temperatures. This version had only one component: an acrylic mold filled with lithium (Fig. 2*A*). First, we demonstrate precise heating by varying the shape of the acrylic channel. The shape of the channel was optimized to increase hydrogen bubble clearance from the channel to improve the interaction between the reactants, lithium and water. We developed lithium-filled acrylic molds with circular, square, triangular, and star-shaped channels of fixed surface area (Fig. 2 *B* and *C* and *SI Appendix*, Fig. S2). These molds were then placed in a cuvette containing 1 mL of water and a tube with contents to be heated. The temperature of the tube was monitored using a thermal camera and hydrogen bubble generation was monitored with a video camera (*SI Appendix*, Fig. S3). The channels with sharper and more numerous angles provided more reproducible temperature profiles and final temperatures (*SI Appendix*, Fig. S2). Circular channels provided the most irregular heating while star-shaped channels provided the most precise and reproducible temperature profiles (Fig. 2 *B* and *C*). This disparity was observed due to the lack of clearance of hydrogen gas from the circular channels, which formed Taylor bubbles (28, 29), or elongated hydrogen bubbles several times longer than the channel diameter. At this size scale, surface tension forces are more predominant over buoyancy forces, which unpredictably impedes rising bubble velocity (28, 30). When the channels are blocked with slower moving Taylor bubbles, less water is able to access the lithium to continuously provide heating. Conversely, with the star-shaped channel, sharper angles resulted in more water being retained in the corners (Fig. 2*D*). With increased retention of water in the corners, more water can move downward and access lithium while still allowing for the clearance of hydrogen bubbles (19). This allows for the reaction to proceed to provide continuous hydrogen bubble generation and precision in heating. We therefore used the precision offered by the star-shaped channels to further build the platform to provide tunable temperatures.

To provide tunability in temperatures, we varied the surface area of the channel openings. This enabled us to vary the amount of water accessing lithium. The surface area of the star-shaped channel from 0.75 mm^2 to 6 mm^2 (~1 to 10 mg) provided a temperature range from ~40 °C to ~100 °C (ΔT_{RT} = ~20 °C to 70 °C) (Fig. 2*E*). Here, we used surface area as a lever to vary the total mass of lithium in the channel, where larger surface areas provided more exposure of lithium to water. Given the high heating rate of the miniature heaters, the total mass of lithium therefore governed the final temperature of the solution (Fig. 2*F*). Surface area of the channel openings was thus used as an indirect physical parameter to tune the final temperature of the solution. In addition to varying the surface area of a channel, it is also possible to provide tunability in temperature by varying the volume of water in which the heater is immersed (*SI Appendix*, Fig. S4). However, the dynamic range provided by this method is not as broad for a given container. We provided precise and a broad range of temperatures by modifying both the shape and surface area of the acrylic channel of the heater.

Improving the Hold-Over Times of the Miniature Heater. We wanted the miniature heater to maintain a range of temperatures within 5 °C of precision for 10 to 15 min (Fig. 3*A*). According to the World Health Organization (WHO), one of the criteria for an ideal test is that it is rapid and robust and can be completed within 30 min (31). Since these tests have multiple steps and require different temperatures, each step can conceivably require a specific temperature to be maintained over 10 to 15 min. To increase hold-over times, we varied the surface tension of the solution to reduce the clearance rate of hydrogen bubbles. By decreasing the hydrogen bubble clearance rate, we were able to decrease the heating rates to prolong and maintain a target temperature in the minute scale. Roughly 70% of the heat generated by the heater is transferred to the sample without the use of any insulation (*SI Appendix*, Figs. S5 and S6). To have hold-over times in the minute scale, we used two heaters: one with a high heating rate and another with a lower heating rate (Fig. 3*A*). The first heater would bring the solution quickly up to a target temperature and the second would maintain the temperature for a period of minutes. To develop a heater with a lower heating rate, the surface tension of the solution in which the heater was immersed was varied by adding different amounts of the surfactant, sodium dodecyl sulfate (SDS) (32, 33). With the inclusion of surfactant, however, we observed a decrease in the peak temperature reached with each subsequent addition of heaters. We hypothesize that this decrease in heating is due to the rate of reaction being reduced by lithium hydroxide (LiOH) byproduct buildup (*SI Appendix*, Fig. S7). We therefore used the maximum volume of 3 mL for experiments which require minute-scale hold-over times to minimize saturation. At this volume, the final temperature of the high heating rate heaters was lower than when in 1 mL solution (*SI Appendix*, Fig. S8). For simplicity, instead of using a high heating rate miniature heater to bring the solution up to a target temperature, we heated the solution to 55 °C (ΔT_{RT} = 30 °C). We then added the low heating rate heater, along with SDS and antifoam to minimize foam formation (34) (Fig. 3*B*). At 1% SDS solution, the temperature of the solution was held constant (±2.5 °C) for 10 min. Below 1% SDS the hold-over times were shorter than 10 min, while above 1% SDS the heating rate was too low to maintain temperature within ±2.5 °C (Fig. 3*B* and *SI Appendix*, Fig. S9). This phenomenon of providing lower heating rates occurs as a result of the interplay between surface tension and hydrogen bubble size. With the addition of surfactant, the surface tension of the solution deceases (32). In a solution of lower surface tension, smaller hydrogen bubbles are generated (35), resulting in slower upward movement (36), greater bubble packing density, and reduced clearance of bubbles (Fig. 3*C*). This in turn decreases the rate of water accessing lithium for consumption, thereby decreasing the heating rate. To further increase hold-over times, we can increase the depth of the acrylic channel. At a constant heating rate, the depth of the channel governs the amount of lithium available for consumption (Fig. 3*E*). We show that there

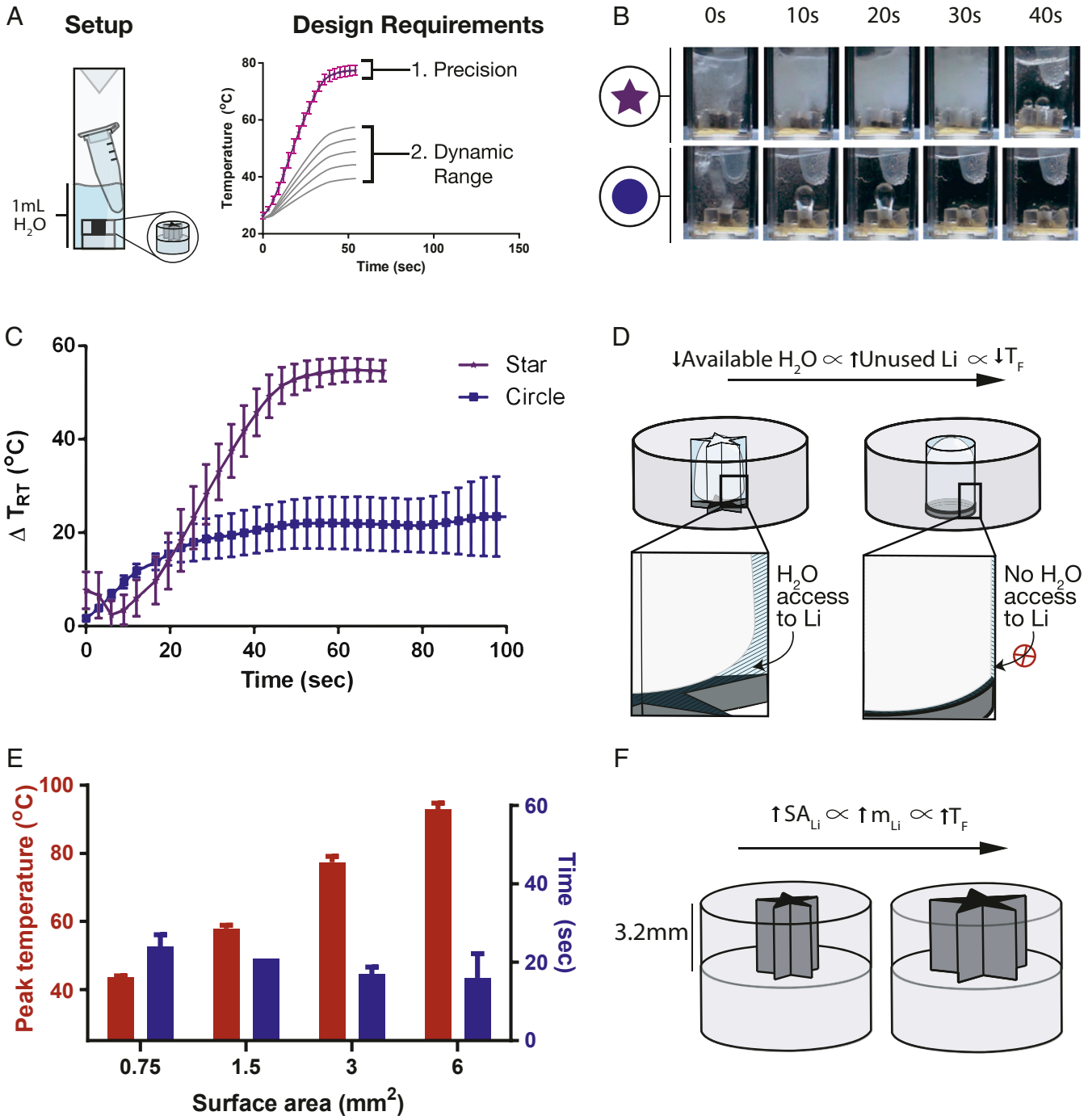

Fig. 2. Effect of shape and surface area on precision and tunability of miniature heaters. (*A*) Design criteria of the miniature heater. We want the heater to be within 5 °C of precision and achieve tunable temperatures in the range of 37 °C to 65 °C (ΔT_{RT} = 12 °C to 40 °C). (*B*) Photographs of miniature heaters with star-shaped vs. circular inner channels in water. Star-shaped inner channels continuously heat the water while clearing hydrogen bubbles, while circular channels result in irregular heating due to lack of hydrogen bubble clearance. Scale of heater: 8 mm. (*C*) Thermal profile of star-shaped vs. circular channeled miniature heaters (n = 3). Star-shaped channels provide precise heating (<5 °C) while circular channels provide irregular heating (>5 °C). (*D*) Mechanism of the role of shape on precise heating. Sharper angled channels can retain more water at their angles and provide access to water despite hydrogen bubble generation. (*E*) Effect of channel surface area on tunability of temperature (n = 3). By varying the surface area of lithium accessing water, the final temperatures can be modulated. (*F*) Mechanism of effect of surface area on final temperatures. Higher surface areas provide larger masses of lithium accessing water to result in higher final temperatures. SA_{Li} = surface area of lithium; m_{Li} = mass of lithium; T_F = final temperature.

is a proportionality between channel depth and hold-over times at a fixed SDS concentration and channel surface area (Fig. 3*F* and *SI Appendix*, Fig. S10). Lastly, we wanted to demonstrate that at the optimal 1% SDS concentration, that we could modulate the temperature of the solution in the minute scale. We varied the surface area of the acrylic channel openings to acquire a range of temperatures that was maintained for ∼10 min (Fig. 3*D*). Here, we show that we can increase hold-over times of the heater by including a surfactant in the solution and varying the depth of the acrylic channel.

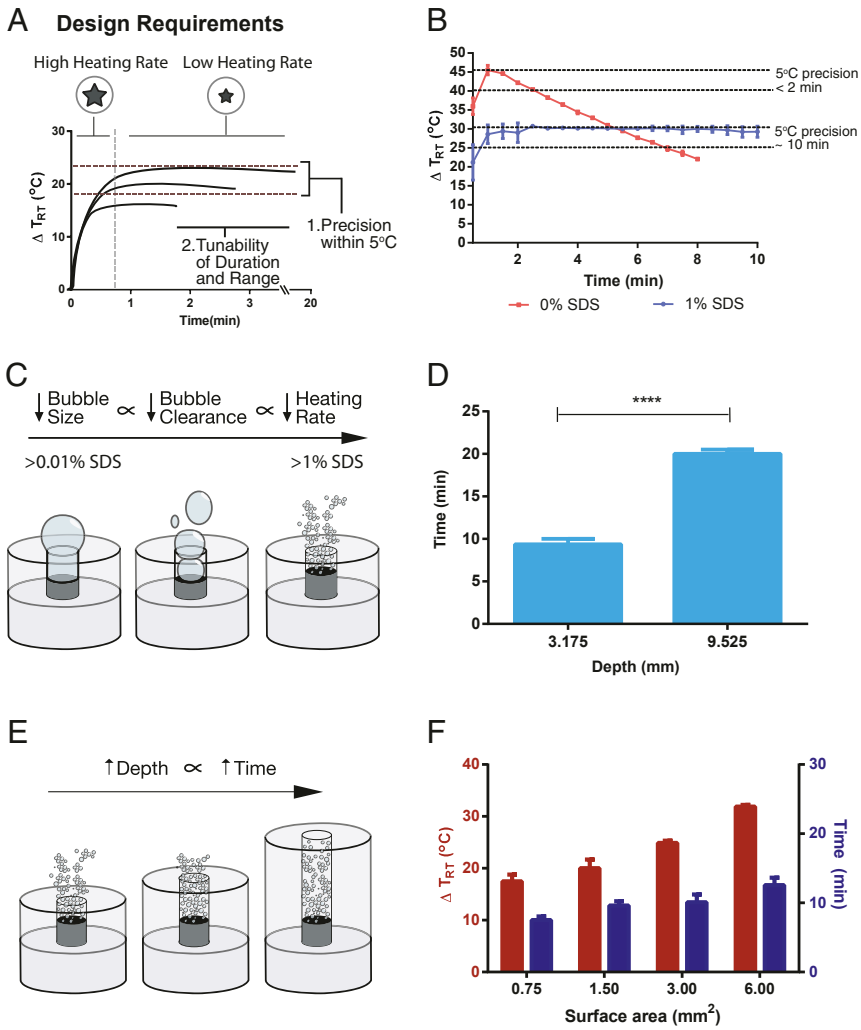

Fig. 3. Factors that govern hold-over times of the miniature heater. (*A*) Design requirements for improving the hold-over times of the heater. Two heaters were used to increase the hold-over times of the heater to 10 to 15 min with 5 °C of precision. (*B*) Effect of surfactant concentration on hold-over times ($n = 3$). Cuvettes with either 0% or 1% SDS were heated to 55 °C ($\Delta T_{RT} = 30$ °C), prior to adding 3-mm^2 star-shaped miniature heater. Hold-over times are determined as the duration of time a temperature is maintained within 5 °C. (*C*) Mechanism by which surfactant increases hold-over times. The introduction of SDS reduces overall bubble size, where smaller hydrogen bubbles rise slower and take longer to clear out of the channel, resulting in slower heating rates. (*D*) Channel depth as a lever to modulate hold-over times. At slower heating rates, channel depth modulates the available lithium for consumption, where mass of lithium is directly proportional to the length of the hold-over time. (*E*) Effect of acrylic channel depth on hold-over times ($n = 3$). The channel depth can be increased to provide longer hold-over times. Statistical significance was calculated with a *t* test (**** = <0.0001). (*F*) Effect of surface area on the tunability of final temperatures on the 10-min time scale ($n = 3$).

Use of Miniature Lithium Heaters in Resource-Limited Settings. We tested for how well the heaters perform in highly humid environments, where performance of the heaters can be drastically reduced, to simulate settings with limited infrastructure. We then tested for how well the heaters deliver reagents while providing safe handling to simulate use by operators with limited training. We tested for the user friendliness of the miniature heaters by first developing the full version of the platform. The full version of the miniature heater includes adding stabilizing excipients to the acrylic mold filled with lithium. To the mold filled with lithium, a ring-shaped acrylic mold was fitted and mineral oil, mannitol, and SDS were added (Fig. 4*A*). First, to test the performance of the heaters in conditions of high humidity, we kept heaters with and without excipients at 20% and 70% relative humidity (RH) for a period of 4 wk. The final temperature reached at each time point when the heater was immersed in water was used as a metric to determine stability. In the presence of excipients, the heaters reached ~55 °C ($\Delta T_{RT} = 30$ °C) for a period of 4 wk while in the absence of excipients the peak temperatures drastically decreased at 20% and 70% RH (Fig. 4*B*). The immiscible nature of mineral oil (25) and non-hygroscopicity of mannitol limit the interaction of lithium with moisture in the air, thereby providing stability. The miniature heaters perform equally well in limited infrastructure environments with lack of controlled humidity.

Next, we demonstrate that the heaters can be used even with limited training. We first show that the miniature heaters can deliver precise amounts of SDS to minimize the overall number of handling steps (Fig. 4*C*). We show that the amount delivered by trained users is comparable in precision to the amount delivered by the heater. Finally, we show that the lithium heaters are safe to handle. We simulated a spill by adding water to equivalent amounts of bare lithium and lithium in the heater. Bare lithium reached a temperature of ~80 °C ($\Delta T_{RT} = 55$ °C) in a matter of seconds while lithium heaters reached a temperature of ~44 °C (~$\Delta T_{RT} = 20$ °C), temperature at which skin burns

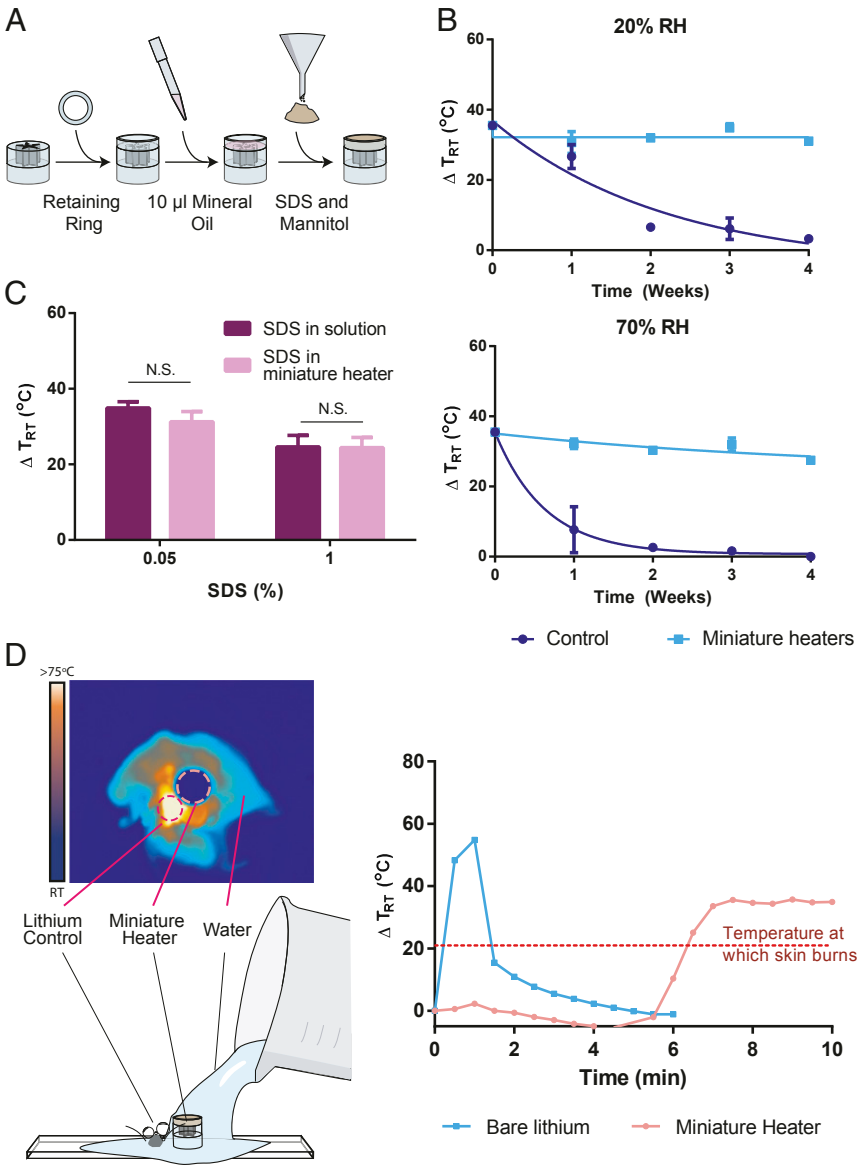

Fig. 4. Demonstrating the user friendliness of the miniature lithium heater. (*A*) Process of adding a soluble mixture of powders and mineral oil. Once lithium is compressed into a mold and sealed at one end, a retaining ring is acetone welded to the other end. To this ring, 10 µL of mineral oil is added, followed by required amounts of SDS and mannitol. (*B*) Stability of the heater at 20% and 70% RH compared to bare lithium ($n = 3$). Heaters retain performance for 4 wk without requiring any additional packaging. (*C*) Comparison of delivering precise amounts of SDS using pipettes vs. with a miniature heater ($n = 3$). A *t* test was conducted to determine statistical significance (N.S., not statistically significant). (*D*) Spill simulation comparing bare lithium to miniature heater ($n = 1$). Representative profile of bare lithium as it reaches high temperatures within a matter of seconds compared to the miniature heater that takes over 6 min, allowing enough time to react to the spill.

occur, in ∼6 min in the absence of agitation (Fig. 4*D*). By using the heater, the end user has a longer period of time to react to a spill and prevent harmful burns. The miniature heaters do not require extensive training to be used.

Demonstrating the Utility of Lithium Heaters in a Diagnostic Assay. We demonstrate the use of the lithium heaters to conduct a generic diagnostic workflow. We show the potential to use the heaters in multistep assays that require different temperatures (*SI Appendix*, Fig. S11). We used T4 bacteriophage as a model system to simulate a clinical sample. We lysed the bacteriophage using heat at 95 °C (ΔT_{RT} = 70 °C), then amplified the DNA at 42 °C (ΔT_{RT} = 17 °C) using recombinase polymerase amplification (RPA) and visualized the DNA using fluorescent assay at 42 °C (ΔT_{RT} = 17 °C) (Fig. 5*A*). For lysis, we used a 6 mm^2 star-shaped heater in 0.05% SDS solution (Fig. 5*B*). The bacteriophage sample was held at 95 °C (ΔT_{RT} = 70 °C) for ∼20 s (*SI Appendix*, Fig. S12). Next, we amplified the lysed DNA using RPA. In RPA, the recombinase proteins form a nuclear-protein complex with primers and scan for homologous sites on the target DNA (37). Once found, the primers bind to the target and strand-exchanging polymerase exponentially amplifies DNA. To conduct RPA, we brought the temperature of the solution up to ∼44 °C (ΔT_{RT} = ∼19 °C) using a 4 mm^2 heater, then maintained the temperature at 42 °C (ΔT_{RT} = 55 °C) for 10 min using a 1.5 mm^2 star-shaped heater at 1% SDS solution (Fig. 5*B* and *SI Appendix*, Fig. S13). After amplification, we visualized the target DNA using a fluorescent assay (38). We used fluorophore-quencher paired probes to first hybridize with amplified DNA. We then used exonuclease III to cleave the probe-DNA hybrid.

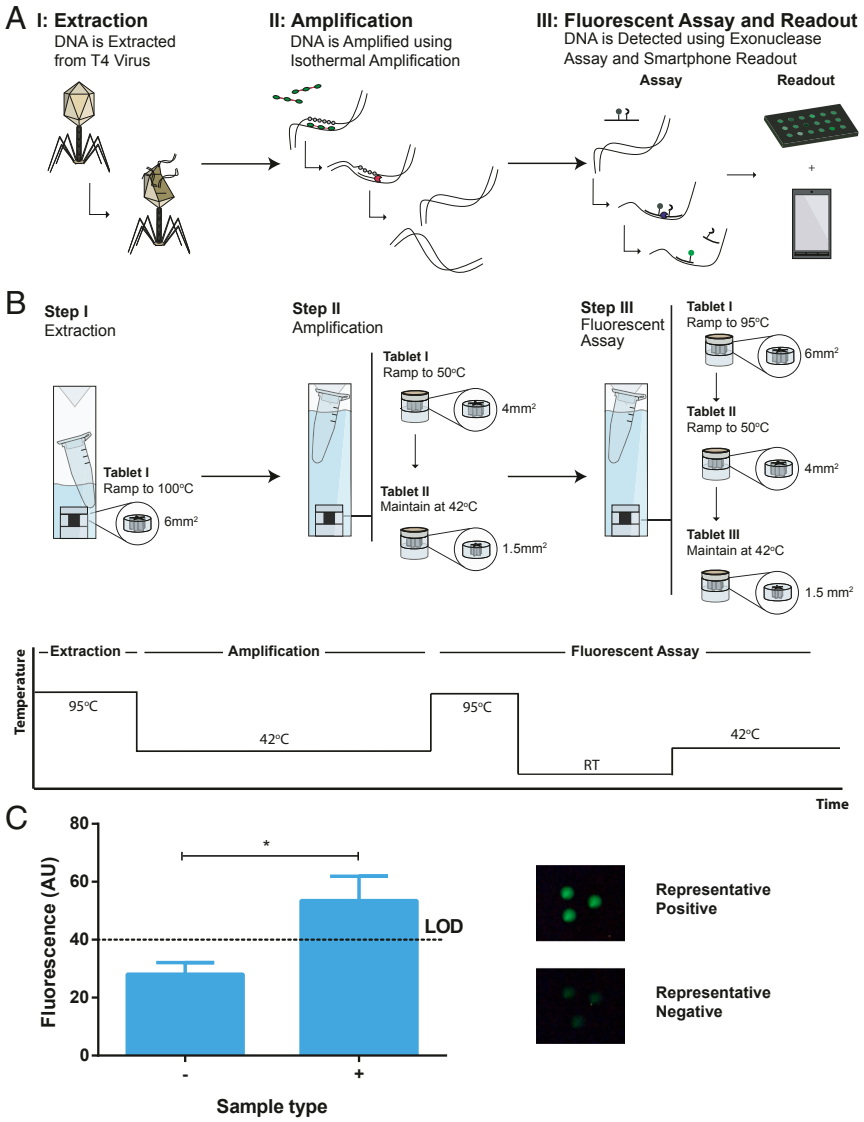

Fig. 5. The use of miniature heaters in a diagnostic workflow. (*A*) Schematic of the diagnostic workflow. (*A*) The workflow involves extraction of DNA from T4 bacteriophage, amplification with RPA and fluorescence detection of the amplified DNA using a smartphone device. (*B*) Schematic showing the combination of heaters required to achieve each temperature. A stepwise temperature curve shows the different temperatures required to complete each step. (*C*) Final fluorescent results of the assay ($n = 3$). Representative images of a positive and a negative result are shown above. Each replicate was analyzed to determine average intensity using ImageJ. LOD, limit of detection. $^*P = 0.0194$.

Cleavage of the probe results in fluorescence as the fluorophore is separated from the quencher (Fig. 5*A*). To conduct the fluorescence assay, we first used a 6-mm^2 heater to bring the temperature up to 95 °C to denature the amplified DNA (Fig. 5*B*). We allowed the solution to cool to room temperature in order for the probes to hybridize with the amplified DNA. We introduced the exonuclease to the reaction and allowed the reaction to incubate at 42 °C (ΔT_{RT} = 55 °C) by adding a 4-mm^2 star heater followed by a 1.5 mm^2. The reaction was allowed to proceed for 10 min. Fluorescence was visualized using a smartphone camera and flashlight paired with an excitation and emission filter. We were able to successfully detect T4 bacteriophage DNA using this workflow with miniature heaters (Fig. 5*C* and *SI Appendix*, Fig. S14).

Discussion

We have developed a reproducible, stable, and safe platform for precise and electricity-free heating of biological assays. We designed each device to be small enough to fit on a fingertip by controlling the interplay between lithium and elongated bubble motion in tubes during the exothermic lithium–water reaction. Each device is made by compressing lithium into various acrylic channels and sealing with a mixture of powders and mineral oil while keeping the overall size under 0.5 cm^3. This approach allows the miniature heaters to be electricity free and reach target temperatures in 1 min while being precise (5 °C) and tunable in the range of biological assays (ΔT_{RT} = 12 °C to 40 °C). Given its small footprint, electricity-free operation, short ramp-up times, precision and tunability, this platform can be used at the point of care to perform biological assays with complex temperature requirements. By introducing a surfactant into the reaction mixture, we can have hold-over times of >20 min. We therefore extend the application of miniature heaters to a range of biological assays. In order to fully realize the potential of the platform for different low-resource environments at the point of care, we show the heaters' stability at 20% and 70% RH for 1 mo. This

addresses typical barriers surrounding environmental control and cold-chain storage encountered in low-resource settings.

Miniature lithium heaters are advantageous over existing technologies for four main reasons: 1) its size, 2) flexibility in temperature modulation, 3) fast ramp-up times, and 4) affordability. Firstly, the size scale of the miniature heater allows for ease of transportation and handling. Approximately 480 miniature heaters can be packaged into a typical 12-oz coffee cup, making it highly portable and easy to conduct complex biological procedures in electricity-free environments. Typical PCMs can be up to anywhere from 10 to 9,000 times larger (8–10, 12, 17) making them less flexible for point of care use. Secondly, its flexibility in temperature tunability allows the platform to be agnostic of the final assay use case, where diverse sets of enzymes are no longer inhibited by the lack of heating infrastructure. Conventional chemical heaters often use PCMs, making it harder to change reaction temperature for different steps in an assay, as this may require reengineering of the device design (12) Obtaining multiple specific and unconventional reaction temperatures within one assay may also prove difficult as you will need to carry multiple PCMs and their associated bulky devices. This is due to PCM's reliance on material-specific properties that result in narrow temperature bounds of each PCM/device combination. The tunability offered by our platform provides the possibility of using this platform for any enzymatic reaction. Thirdly, our heater can achieve target temperatures in 1 min, which is 5 to 30 times faster (8) than current chemical heaters. This reduces the amount of time for results. For example, for a typical 30-min amplification reaction that would otherwise require a 10-min ramp-up time, using a miniature heater would decrease the overall assay time by ∼30%, enabling quick turnaround and response times. Lastly, miniature heaters are inexpensive to use. Each heater costs around ∼7 cents per reaction (*SI Appendix*, Table S3). For 100 reactions, this would require a material cost of ∼US$7. For conventional chemical heaters on the other hand, the PCM itself can cost up to ∼US$54/kg (39) with recurring reagent costs for fuel source replenishments. Our miniature heaters are a competitive alternative for use in electricity-free settings.

However, to be fully ready for deployment in the field, further improvements to the miniature heater are required. First, the byproducts of the reaction, both hydrogen gas and lithium hydroxide, may be a cause for concern for a lay user. For a typical heater that has ∼2 to 20 mg of lithium, ∼0.29 to ∼2.9 mg of hydrogen gas is produced. The lower explosive limit or the minimum concentration of hydrogen gas required to support combustion is 4% by volume (40). At a maximum mass of 2.9 mg and density of 0.09 g/L, this would require the testing space to be enclosed and smaller than the size of a large bottle of water (∼800 cm^3 by volume) to result in an explosion in the presence of an ignition source. In a well-ventilated space, we do not foresee this amount of hydrogen gas generated per even multiple reactions to be problematic. On the other hand, for a similar mass of lithium, ∼0.29 to 2.9 M of lithium hydroxide is produced. At this concentration of lithium hydroxide, the solution can reach a pH of 13 to 14, which is caustic in case of a spill. For future iterations of the miniature heater, we envision implementing the capability to carry a neutralizing chemical such as ascorbic acid to facilitate safer handling. Lastly, from an applications perspective, although we have shown the utility of miniature heaters for diagnostic purposes, we could use it for anything from cooking and boiling water to gene editing. The byproducts from this reaction could be harnessed for other uses. This could range anywhere from using hydrogen gas as a propellent for small-scale reactions to providing electricity via fuel cells at the point of care. Ultimately, we envision providing better access to cutting edge biochemical techniques including diagnostics, by making portable and electricity-free heating available at any location.

Materials and Methods

Development of Miniature Lithium Heaters. A total of 0.75 mm^2 to 6 mm^2 stars were created in Illustrator and transferred to RetinaEngrave software. Acrylic sheets (3.175 mm) (McMaster-Carr) were laser cut (Full Spectrum Laser) with an inner shape of varying surface area (0.75 mm^2 to 6 mm^2) using RetinaEngrave software. The resulting area will depend on the manufacturing tolerance. Next, a 9-mm diameter outer circular shape was laser cut using the same method. This was used as the acrylic mold to which lithium wires (Sigma-Aldrich) were compressed using manual compression. In the future, we envision increasing the throughput of development by using a rotary tablet press for compression. Excess lithium was shaved off and one end of the mold was sealed with an additional acrylic cylinder 9 mm in diameter. Sealing was done by using acetone to melt the acrylic base prior to attaching to the lithium-filled mold. The acrylic base and the lithium-filled mold comprised the simple version of the miniature heater. To develop the full version of the heater, 1.5875-mm acrylic sheets (McMaster-Carr) were laser cut into ring shapes with an inner diameter of 7 mm and outer diameter of 9 mm. Using the same sealing method, the rings were attached to the mold. Finally, 10 μL of mineral oil (BioShop), variable amounts of SDS (Medstore), and mannitol (Mannogem EZ spray-dried mannitol, SPI Pharma), depending on heating rate preferred, were added to the ring-shaped mold.

Development of Different Channel Shapes to Provide Precision in Heating. Different shapes of 3 mm^2 were laser cut as previously described. The triangle was equilateral while the star was composed of five isosceles triangles with an acute angle at the tip of 30°. The acrylic channels were filled with lithium and sealed at the bottom as previously described. To monitor temperature, the molds were placed upright in 1 mL of water using a 4-mL cuvette (BioMart, catalog no. 112804). To the cuvette, a 600-μL Eppendorf was placed with 50 μL of reaction volume to be heated. A thermal camera (FLIR E60) was then used to monitor the temperature of the reaction volume in the Eppendorf. Using FLIR Tools$^+$ software, we were able to acquire the temperature of the solution over time. We monitored hydrogen bubble motion through channels using a video camera.

Development of Different Channel Surface Areas to Provide a Range of Temperature (High Heating Rate). Stars with surface area of 0.75 mm^2, 1.5 mm^2, 3 mm^2, and 6 mm^2 were laser cut and developed into a simple version of the heater as previously described. The heaters were placed in 1 mL of water. Heating provided by the heaters was monitored with a thermal camera by placing an open Eppendorf tube with 50 μL of water. The resulting temperature of each heater was calculated by the peak temperature recorded. Duration at which the peak temperature was maintained was determined by the period of time at which temperature was within 5 °C.

Use of SDS to Increase Hold-Over Times. The 3 mm^2 star-shaped channeled molds were filled with lithium and sealed on one end using another acrylic mold. Three-millimeter solutions of 0%, 0.5%, 1%, and 2% SDS with 5% silicone antifoam (Sigma-Aldrich, lot no. BCBZ4425) were made. The solutions were first heated using a water bath up to 55 °C, at which point the miniature heaters were dropped into the solution. Temperature over time was monitored by placing a PCR tube with 50 μL of water.

Development of Different Channel Surface Areas to Provide a Range of Temperatures (Low Heating Rate). Simple versions of the heaters were developed with star-shaped channels with surface areas of 0.75, 1.5, 3, and 6 mm^2. Cuvettes with 3 mL of 1% SDS and 10% silicone antifoam (the amount antifoam added varied depending on the effectiveness of the lot) were prepared. The temperatures of the cuvettes were increased to either 44 °C, 49 °C, 55 °C, or 59 °C, respectively (using a water bath) for each respective surface area. At the increased temperature, the heaters were placed in the cuvettes and the temperature was monitored (of a PCR tube with 50 μL of water) using a thermal camera. Peak temperatures were determined as the maximum temperature reached by each heater. Duration was calculated by determining the period of time a target temperature was maintained within 5 °C.

Development of Longer Channel Depths to Prolong Hold-Over Times. The 1.5-mm^2 star-shaped channel molds with a depth of 3.175 mm were developed into simple heaters. To develop a simple heater with a depth of 9.525, three individual 1.5-mm^2 star-shaped molds were first filled with lithium. The three molds were melted on one end with acetone and fixed atop one another, similar to a building made out of building blocks and sealed at one

end. Monitoring and measurement of temperature and duration were performed as previously described.

Moisture Stability Study. Miniature heaters with and without (control) mineral oil and mannitol were developed and stored at 20% RH or 70% RH. Control and miniature heaters were developed by laser cutting 1.5 mm^2 star-shaped channels from 3.175-mm acrylic sheets. These molds were then filled with lithium. Cylindrical molds used for the bottom seal were laser cut using 3.175-mm acrylic sheets with a diameter of 8 mm. Ring-shaped molds to be fixed atop were laser cut with 1.5875-mm acrylic sheets, with an outer diameter of 8 mm and inner diameter of 6 mm. The ring-shaped molds and the lithium-filled molds were kept in acetone for 20 min while the bottom seal molds were kept in acetone for 40 min. Control as well as the miniature heaters were developed by fixing the bottom seal, lithium-filled mold, and ring-shaped mold together. To the miniature heater (unlike the controls) 10 μL of mineral oil was added and topped with mannitol. To test the final temperature of the solution, the controls as well as the miniature heater were placed in 1 mL of 0.05% SDS and 10% silicone antifoam. The peak temperature was monitored every week for 4 wk with an Eppendorf tube with 50 μL of water.

Using Heaters to Carry SDS/Mannitol. The 1.5-mm^2 stars with an outer diameter of 9 mm were laser cut using a 3.175-mm acrylic sheet. The bottom seal (3.175-mm acrylic sheet) was laser cut to have a diameter of 9 mm while the ring-shaped mold (1.5875-mm acrylic sheet) had an outer diameter of 9 mm and inner diameter of 7 mm. The three components were sealed together by using acetone (on the bottom seal and the ring-shaped molds) to slightly melt the acrylic. To this design, 10 μL of mineral oil was added. For three replicates, 30 mg of SDS was added (1% SDS) while to another set of three replicates, 0.5 mg of SDS and 29.5 mg of mannitol were added (0.05% SDS). Monitoring and measurement of temperature and duration were performed as previously described.

Spill Simulation Test. A 1.5-mm^2 star-shaped channel with an outer diameter of 9 mm was laser cut and developed into the full version of a miniature heater as previously described. Filled and empty versions of the channel were compared to determine the amount of lithium each heater contained. An equivalent amount of lithium, 5.63 ± 0.21 mg, was weighed and placed beside the heater on a glass slide. A total of 500 μL of water was measured and poured onto the glass slide while being recorded by the thermal camera. The temperature profile of peak temperatures reached by the lithium and by the miniature heater was monitored over a 10-min time period.

Propagation of T4 Phages. A total of 10 mL of 20 g/L LB was inoculated with *Escherichia coli* (ATCC, catalog no. 11303) and cultured overnight at 37 °C. A total of 20 mL of 1.5% agar in LB was added to Petri dishes and allowed to solidify. A total of 10 μL of T4 phages (ATCC) was added and mixed with 200 μL of cultured *E. coli*. This mixture was added to 5 mL of 0.5% agar in LB. The phage/bacteria/agar mixture was added to the Petri dishes with 1.5% agar and left overnight at 37 °C for propagation. After overnight incubation, the soft agar was scraped and included in 30 mL of LB. The solid debris was spun down at 1,000 × *g* for 25 min and supernatant with T4 phage colonies (filtered with a 0.22-μm filter) was used for the diagnostic workflow.

Centrifugation of T4 Phages. In order to remove free-floating DNA from T4 phage samples, the samples were spun down at 20,000 × *g* for 90 min. The supernatant was then removed and the pellet was resuspended in equivalent volumes of 50 mM Tris and 10 mM $MgCl_2$ at pH 7.5. The solution was left overnight at 4 °C to allow for resuspension without vigorous agitation.

Lysis of T4 Phages. The 6-mm^2 star-shaped channels were laser cut and developed into a full version of the heater. To the final design, 10 μL of mineral oil, 0.5 mg of SDS, and 29.5 mg of mannitol were added. T4 phages were diluted 1:100 in 50 mM Tris and 10 mM $MgCl_2$ at pH 7.5. Three replicates of 80 μL of the diluted phages were placed in a cuvette with 1 mL of water, along with the developed heater and 10% silicone antifoam. Controls were run side by side, where 80 μL of diluted T4 phages were lysed at 95 °C for 1 min using a thermal cycler. The amount of lysed DNA was qualitatively measured by mixing 10 μL of lysed sample with 190 μL of 1× SYBR Gold. Fluorescence was measured using a plate reader (Tecan Life Sciences).

RPA Sample Preparation. For each replicate, the following premix was made (volumes are for single replicates): 2.4 μL of 10 μM forward primer (5′ TGATTTACAAGAATTGCGAATGGTGCTTGTTCATC 3′), 2.4 μL of 10 μM reverse primer (5′ AGTGGAAACTGAAACTCGATAATGCGGGTAACGG 3′) (Integrated DNA Technologies), 9.2 μL of water, 29.5 μL of rehydration buffer, and 2.5 μL of 280 mM MgAc (Abbott Laboratories). To 46 μL of the premix, an RPA pellet was added along with 40 μL of water (negative control) or 40 μL of unpurified lysed T4 DNA.

RPA of Lysed T4 Phages Using Miniature Heaters. To run RPA at 42 °C, 4 mm^2 (gets up to 50 °C) and 1.5-mm^2 (maintains at 42 °C) star-shaped heaters were developed. To the 4-mm^2 heater, 1.5 mg of SDS and 28.5 mg of mannitol were added. To the 1.5-mm^2 heater, 30 mg of SDS was added. The heaters were placed in 3 mL of water (4 mm^2 first followed by 1.5-mm^2 heater) and 10% silicone antifoam. PCR tubes with RPA reaction mixture (either negative for DNA or with unpurified lysed T4 DNA) were placed in the cuvette. The RPA reaction was allowed to proceed for 10 min. Amplified products were visualized using a 3% agarose gel and visualized with GreenDNA Dye (BioBasic) and a gel scanner (Gel Doc EZ Gel).

Fluorescence Assay.

Sample preparation for denaturation. To 50 μL of the amplified product (both negative control and sample), 0.6 μL of 10 μM exo probe was added. We used the following sequence for the exo probe: 5′TCAAGCAGTAATTCGTTT(dT-6FAM) (dSpacer) (dT-BHQ1)TCCGTCTAAAAAT3′ (BioBasic).

Denaturation step. The 6-mm^2 star-shaped molds were developed into miniature heaters. To the heaters, 0.5 mg of SDS and 29.5 mg of mannitol were added. The heaters were placed in 1 mL of water and 10% silicone antifoam to bring the temperature of the solution up to 95 °C. The samples in PCR tubes with the exo probes were placed in the cuvette and allowed to be denatured for less than 1 min. The probes were allowed to be denatured for less than 1 min. The probes were then allowed to hybridize with amplified product by leaving the reaction tube at room temperature for 10 min.

Sample preparation for cleavage with exonuclease III. To the probe-amplified DNA product, 5 μL of 10× exonuclease III reaction buffer as well as 0.5 μL of 200 U/μL exonuclease II were added (Thermo Fisher Scientific).

Cleavage with exonuclease III. To run the fluorescence assay at 42 °C, a heater with 4-mm^2 star-shaped channel and 1.5-mm^2 star-shaped channel were developed. To the 4-mm^2 heater, 1.5 mg of SDS and 28.5 mg of mannitol were added; while the 1.5-mm^2 heater had 30 mg of SDS. The 4-mm^2 heater was first placed in 3 mL of water and 10% antifoam. The lithium was allowed to be fully consumed, after which the 1.5-mm^2 heater was placed in the solution to maintain the temperature at 42 °C. To the cuvette, PCR tubes with amplified products, probes, and exonuclease III were placed in solution. The reaction was allowed to proceed for 10 min.

Detection of Fluorescence with Smartphone Device. A holder for an iPhone SE was three-dimensionally (3D) printed to hold a 536/40 emission filter. A 465-nm flashlight (Joyland; part no. CSK68B) with a 480/40 excitation filter was used as an excitation source. The phone holder and flashlight were fixed relative to each other and the sample using a retort stand. Images were acquired using the application NightCap at International Organization of Standardization's (ISO) measure of sensor sensitivity of 4000 units, and 10-s exposure at 1/2-s exposure per frame. Images were saved as .jpg format and mean intensity was analyzed on ImageJ. A two-tailed *t* test was conducted to determine if the positives and negatives were statistically significant.

Data Availability. All data are included in the manuscript and *SI Appendix*.

ACKNOWLEDGMENTS. We thank Dr. Abdullah Muhammad Syed for reading and providing feedback on our manuscript and Ben Kingston for photography. W.C.W.C. acknowledges the Canadian Institutes of Health Research and Natural Sciences and Engineering Research Council of Canada through the Collaborative Health Research Program (CPG-158269 and 2015-06397). B.U. acknowledges the Natural Sciences and Engineering Research Council of Canada Postgraduate Scholarship, the Barbara and Frank Milligan Graduate Fellowship, the Paul Cadario Doctoral Fellowship in Global Engineering, and McCuaig-Throop Bursary for support. P.K. acknowledges the Barbara and Frank Milligan Graduate Fellowship for support. W.C.W.C. acknowledges the Canadian Research Chairs Program (950-223824).

1. J. R. Choi *et al*., Sensitive biomolecule detection in lateral flow assay with a portable temperature-humidity control device. *Biosens. Bioelectron.* **79**, 98–107 (2016).
2. B. L. Fernández-Carballo *et al*., Low-cost, real-time, continuous flow PCR system for pathogen detection. *Biomed. Microdevices* **18**, 34 (2016).
3. J. Singleton *et al*., "Instrument-free exothermic heating with phase change temperature control for paper microfluidic devices" in *Proceedings SPIE International Society Optical Engineering* (Society of Photo-optical Instrumentation Engineers, Bellingham, WA 2013), vol. 8615, pp. 86150R.

4. D. Farquharson, P. Jaramillo, C. Samaras, Sustainability implications of electricity outages in sub-Saharan Africa. *Nat. Sustainability* **1**, 589–597 (2018).
5. The World Bank, Data from "Access to electricity (% of population)." The World Bank. https://data.worldbank.org/indicator/EG.ELC.ACCS.ZS. Accessed 13 August 2019.
6. M. Urdea *et al*., Requirements for high impact diagnostics in the developing world. *Nature* **444** (suppl. 1), 73–79 (2006).
7. S. Sharma, J. Zapatero-Rodríguez, P. Estrela, R. O'Kennedy, Point-of-Care diagnostics in low resource settings: Present status and future role of microfluidics. *Biosensors (Basel)* **5**, 577–601 (2015).
8. J. R. Buser *et al*., Precision chemical heating for diagnostic devices. *Lab Chip* **15**, 4423–4432 (2015).
9. L. K. Lafleur *et al*., A rapid, instrument-free, sample-to-result nucleic acid amplification test. *Lab Chip* **16**, 3777–3787 (2016).
10. R. Snodgrass *et al*., A portable device for nucleic acid quantification powered by sunlight, a flame or electricity. *Nat. Biomed. Eng.* **2**, 657–665 (2018).
11. K. A. Curtis *et al*., Isothermal amplification using a chemical heating device for point-of-care detection of HIV-1. *PLoS One* **7**, e31432 (2012).
12. K. G. Shah *et al*., Design of a new type of compact chemical heater for isothermal nucleic acid amplification. *PLoS One* **10**, e0139449 (2015).
13. J. P. Goertz *et al*., Multistage chemical heating for instrument-free biosensing. *ACS Appl. Mater. Interfaces* **10**, 33043–33048 (2018).
14. R. M. Daniel, M. J. Danson, Temperature and the catalytic activity of enzymes: A fresh understanding. *FEBS Lett.* **587**, 2738–2743 (2013).
15. New England Biolabs, NEBuffer activity/performance chart with restriction enzymes | NEB. https://international.neb.com/tools-and-resources/usage-guidelines/nebuffer-performance-chart-with-restriction-enzymes. Accessed 13 August 2019.
16. Y. Chander *et al*., A novel thermostable polymerase for RNA and DNA loop-mediated isothermal amplification (LAMP). *Front. Microbiol.* **5**, 395 (2014).
17. P. LaBarre *et al*., A simple, inexpensive device for nucleic acid amplification without electricity-toward instrument-free molecular diagnostics in low-resource settings. *PLoS One* **6**, e19738 (2011).
18. D. W. Jeppson, J. L. Ballif, W. W. Yuan, B. E. Chou, *Lithium literature Review: Lithium's Properties and Interactions* (Hanford Engineering Development Lab, 1978).
19. Q. Liao, T. S. Zhao, Modeling of Taylor bubble rising in a vertical mini noncircular channel filled with a stagnant liquid. *Int. J. Multiph. Flow* **29**, 411–434 (2003).
20. H. Liu, C. O. Vandu, R. Krishna, Hydrodynamics of taylor flow in vertical capillaries: Flow regimes, bubble rise velocity, liquid slug length, and pressure drop. *Ind. Eng. Chem. Res.* **44**, 4884–4897 (2005).
21. Z.-S. Mao, A. E. Dukler, The motion of Taylor bubbles in vertical tubes. I. A numerical simulation for the shape and rise velocity of Taylor bubbles in stagnant and flowing liquid. *J. Comput. Phys.* **91**, 132–160 (1990).
22. G. Xiang, X. Zhang, C. An, C. Cheng, H. Wang, Temperature effect on CRISPR-Cas9 mediated genome editing. *J. Genet. Genomics* **44**, 199–205 (2017).
23. T. Araki, The effect of temperature shifts on protein synthesis by the psychrophilic bacterium Vibrio sp. strain ANT-300. *J. Gen. Microbiol.* **137**, 817–826 (1991).
24. A. Farewell, F. C. Neidhardt, Effect of temperature on in vivo protein synthetic capacity in Escherichia coli. *J. Bacteriol.* **180**, 4704–4710 (1998).
25. A. V. Rawlings, K. J. Lombard, A review on the extensive skin benefits of mineral oil. *Int. J. Cosmet. Sci.* **34**, 511–518 (2012).
26. H. L. Ohrem, E. Schornick, A. Kalivoda, R. Ognibene, Why is mannitol becoming more and more popular as a pharmaceutical excipient in solid dosage forms? *Pharm. Dev. Technol.* **19**, 257–262 (2014).
27. B. Udugama, P. Kadhiresan, A. Samarakoon, W. C. W. Chan, Simplifying assays by tableting reagents. *J. Am. Chem. Soc.* **139**, 17341–17349 (2017).
28. P. Angeli, A. Gavriilidis, Hydrodynamics of taylor flow in small channels: A review. *Proc. Inst. Mech. Eng. Part C J. Mech. Eng. Sci.* **222**, 737–751 (2008).
29. W. Salman, A. Gavriilidis, P. Angeli, On the formation of Taylor bubbles in small tubes. *Chem. Eng. Sci.* **61**, 6653–6666 (2006).
30. E. E. Zukoski, Influence of viscosity, surface tension, and inclination angle on motion of long bubbles in closed tubes. *J. Fluid Mech.* **25**, 821–837 (1966).
31. WHO, Low-cost tools for diagnosing and monitoring HIV infection in low-resource settings. https://www.who.int/bulletin/volumes/90/12/BLT-12-102780-table-T1.html. Accessed 10 September 2019.
32. F. H.-B. de Castro, A. Gálvez-Borrego, M. C. Hoces, Surface tension of aqueous solutions of sodium dodecyl sulfate from 20 °C to 50 °C and pH between 4 and 12. *J. Chem. Eng. Data* **43**, 717–718 (1998).
33. K. J. Mysels, Surface tension of solutions of pure sodium dodecyl sulfate. *Langmuir* **2**, 423–428 (1986).
34. N. D. Denkov, Mechanisms of foam destruction by oil-based antifoams. *Langmuir* **20**, 9463–9505 (2004).
35. M. Asari, F. Hormozi, *Experimental Determination of Bubble Size in Solution of Surfactants of the Bubble Column* (Global Journal of Research In Engineering, 2014).
36. S. H. Park, C. Park, J. Lee, B. Lee, A simple parameterization for the rising velocity of bubbles in a liquid pool. *Nucl. Eng. Technol.* **49**, 692–699 (2017).
37. O. Piepenburg, C. H. Williams, D. L. Stemple, N. A. Armes, DNA detection using recombination proteins. *PLoS Biol.* **4**, e204 (2006).
38. J.-C. Wang, L.-B. Liu, Q.-A. Han, J.-F. Wang, W.-Z. Yuan, An exo probe-based recombinase polymerase amplification assay for the rapid detection of porcine parvovirus. *J. Virol. Methods* **248**, 145–147 (2017).
39. J. Kosny, N. Shukla, A. Fallahi, "Cost analysis of simple phase change material-enhanced building envelopes in southern U.S. Climates" (Rep. DOE/GO-102013-3692, National Renewable Energy Laboratory, Golden, CO 2013).
40. L. I. Ji-bo, L. Dong, C. Zhen-zhong, The research on combustible gas lower limit of explosion expanding in high temperature. *Procedia Eng.* **11**, 216–225 (2011).